Available online at www.sciencedirect.com
ScienceDirect
Scripta Materialia 62 (2010) 179–182
Scripta MATERIALIA
www.elsevier.com/locate/scriptamat

Surface segregation in nanoparticles from first principles: The case of FePt

Roman V. Chepulskii,[a,*] W.H. Butler,[b] A. van de Walle[c] and Stefano Curtarolo[a,*]

[a]*Department of Mechanical Engineering and Materials Science, Duke University, Durham, NC 27708, USA*
[b]*Center for Materials for Information Technology, University of Alabama, Tuscaloosa, AL 35487, USA*
[c]*Division of Engineering and Applied Science, California Institute of Technology, Pasadena, CA 91125, USA*

Received 11 September 2009; revised 12 October 2009; accepted 14 October 2009
Available online 17 October 2009

FePt nanoparticles are known to exhibit reduced $L1_0$ order with decreasing particle size. The phenomenon is addressed by investigating the thermodynamic driving forces for surface segregation using a local (inhomogeneous) cluster expansion fit to ab initio data. Subsequent Monte Carlo simulations reveal that first surface layer Pt segregation is compensated by Pt depletion in the second subsurface layer. This indicates that the core's ordered state is not affected by surface thermodynamics as much as previously thought. Published by Elsevier Ltd. on behalf of Acta Materialia Inc.

Keywords: Nanocrystalline materials; Magnetic anisotropy; Surface segregation; Monte Carlo techniques; Cluster expansion

Understanding the physics of the transition from bulk to nanoscale magnetic alloys is important from both a fundamental [1–3] and a technological point of view. In the last decade, Fe–Pt nanoparticles have been intensively investigated in view of possible future applications as an ultra-high-density information-storage medium and high-performance permanent magnets [4–13]. The critical issue for information-storage application is the presence of magnetic anisotropy offering sufficiently large thermal stability. In Fe–Pt, a high magnetic anisotropy is guaranteed by an ordered $L1_0$ phase. However, recent experimental observations have shown a difficulty in obtaining a high degree of $L1_0$ order in FePt nanoparticles annealed at $T \lesssim 600\,^{\circ}\mathrm{C}$ with diameter less than ~4 nm [8–10,14]. Due to the high surface to volume ratio of nanoparticles, surface segregation has been suggested to be one of the possible causes of this reduced ordering [15–20] (interestingly, in FeC and FeMoC nanoparticles, size plays the opposite role, inducing a disorder–order transition [22,23]).

In this letter, we address the FePt surface segregation problem with accurate ab initio computational thermodynamics techniques. In earlier studies, the phenomenon was tackled using several interatomic model potentials [17–21]. Pair interactions were fitted to the experimental phase diagram [17–20] and to bulk first-principles data [17,18]. A single-layer isotropic surface potential was estimated from the surface energy difference between pure face-centered cubic) fcc Fe and Pt [17,18] and by fitting to experimental segregation profiles [19,20]. The embedded atom method potential was used in Ref. [21]. More recently, surface segregation in small Fe–Pt clusters was studied by direct comparison of the energies of several different configurations obtained from first principles [24]. Our approach is radically different: the surface potential is obtained from ab initio calculations without fitting to experimental data and without a priori assumptions about strength and isotropy. We combine the surface potential obtained using the method just described and the bulk pair potential [15,16] into a local (inhomogeneous) cluster expansion [25–27], enabling efficient Monte Carlo simulations to describe the nanoparticle's actual thermodynamic equilibrium segregation profile. The temperature and size dependencies of the $L1_0$ order identify the regimes when surface segregation is responsible for reduced equilibrium order with correspondingly low magnetic anisotropy.

The nanoparticle is modeled as an fcc-based "truncated octahedron" (Fig. 1), which is typically observed for chemically synthesized FePt nanoparticles [1–3,28–30] with free boundary conditions. The initial atomic configuration is considered as ordered $L1_0$ with alternating Fe and Pt layers forming (001) fcc crystal planes. This particle has three inequivalent types of surfaces, (001), (100) and (111), which are addressed by using standard periodic slab geometries (Fig. 1). The vacuum layer thickness was chosen to be approximately equal to

* Corresponding authors. E-mail: r_chepulskii@yahoo.com; stefano@duke.edu

1359-6462/$ - see front matter Published by Elsevier Ltd. on behalf of Acta Materialia Inc.
doi:10.1016/j.scriptamat.2009.10.019

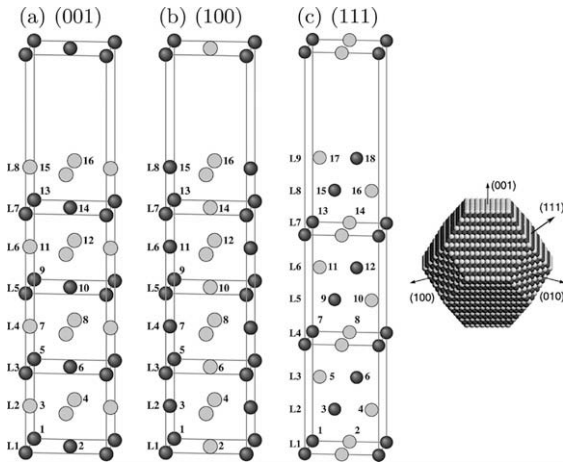

Figures 1. The unit cells of crystal structures representing atomic slabs separated by vacuum used to model the nanoparticle's facets. Each slab is obtained from an unrelaxed $L1_0$ crystal structure along (a) (0 0 1), (b) (1 0 0) and (c) (1 1 1) planes. Layers (L) and atoms are labeled with num- bers. Fe and Pt atoms are represented as black and grey circles, respectively.

three fcc lattice parameters. As well as perfectly ordered slabs, defected surfaces obtained by exchange(s) of atoms belonging to different atomic layers are considered. The energies were calculated from first principles within the generalized gradient approximation using projector-augmented wave pseudopotentials, as implemented in the VASP package [31–33]. The calculated slab energy differences are presented in Figure 2. In agreement with previous theoretical [17,18,21,24,34,35] and experimental reports [36–39], the data indicate that there is an energetic gain for Pt atoms to segregate into all three considered surfaces.

To parameterize the energetic contribution to surface segregation, a number of local cluster expansions (LCEs) are constructed so that they reproduce atom exchange energies obtained from total energy calculations both in the bulk and in the surfaces. The local (or inhomogeneous) nature of the cluster expansions (CEs) manifests itself by the presence of a layer-dependent unary mixing potential $V^{(1)}$ (see Eqs. (4) and (7) in Refs. [15,16]). Such a layer dependence near the surface may be formally considered as an external surface potential applied to the surface atoms. The constructed LCEs differ from each other by the number of external layers affected by surface potential and by the directional dependence of surface potential. The constructed LCEs and their accuracy in surface regions are presented in Figure 3 and Table 1. The previously proposed bulk CE [15,16] has to be modified only at two external surface layers (see Fig. 3) so that only the LCEs with one and two layers of surface potentials have to be considered. Comparing the prediction errors of different CEs, it is concluded that accounting for surface the potential within the second layer has a larger effect than considering the anisotropy in the surface potential. Hence, we conclude that the "iso2" LCE (with isotropic two-layer surface potential) represents the best compromise between the accuracy and complexity of calculations. Note that the "iso1" surface potential (−0.33 eV) is very similar to the corresponding surface potential (−0.30 eV) obtained in Refs. [17–20] with different approaches.

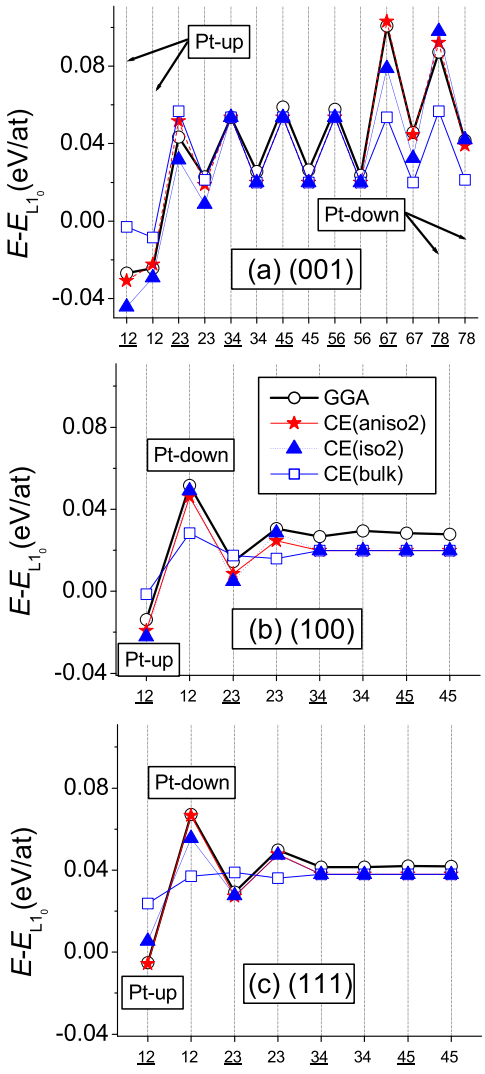

Figures 2. Formation energies of different slabs with respect to ideal $L1_0$ slabs from both first principles (GGA) and using three cluster expansions: "aniso2", "iso2" and "bulk" (see Table 1). The slabs are identified by the label "*ij*", where *i* and *j* indicate the layers between which the atoms are exchanged (Fig. 1). Two configurations are considered: *ij* and $\underline{ij}$ for every choice of *i* and *j*. "Pt-up"/"Pt-down" mean that Pt atoms move to/from the surface of the corresponding perfect $L1_0$ slab, respectively.

The cluster expansion is then employed in a finite-temperature Monte Carlo simulation scheme [15,16], which, during the evolution, produces the free energy of the system. While spanning the phase space, the $L1_0$ order is monitored by the "generalized" parameter $\overline{\eta}$:

$$\overline{\eta} = \left\langle \max\left\{|\eta_x|, |\eta_y|, |\eta_z|\right\} - \min\left\{|\eta_x|, |\eta_y|, |\eta_z|\right\} \right\rangle, \qquad (1)$$

where $\langle \ldots \rangle$ is the statistical average over the Monte Carlo steps, and three directional parameters η_i $(i = x, y, z)$ are defined as the difference between the Pt atom concentrations at odd and even crystal planes perpendicular to the *i*th direction. The generalization is required for small nanoparticles because, in the presence of a surface potential, we have observed that all η_i can be comparable in wide temperature intervals. Generally, we cannot neglect $\min\{|\eta_x|, |\eta_y|, |\eta_z|\}$ in Eq. (1) as was done in Refs. [15,16]. In the case of isotropic order, $|\eta_x| = |\eta_y| = |\eta_z|$, we have $\overline{\eta} = 0$.

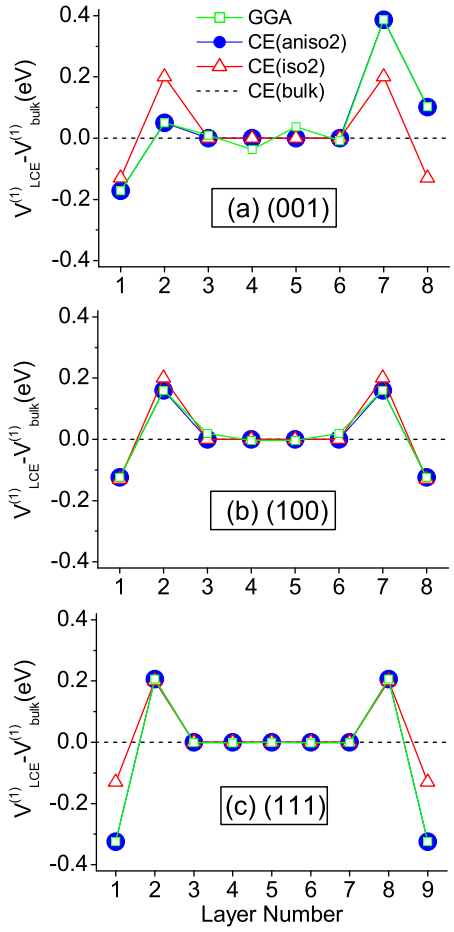

Figures 3. The dependence of surface potential $V^{(1)}_{\mathrm{LCE}} - V^{(1)}_{\mathrm{bulk}}$ on the layer number in (a) (0 0 1), (b) (1 0 0) and (c) (1 1 1) slabs corresponding to initial first-principles (GGA) data and three cluster expansions: "aniso2", "iso2" and "bulk" (see Table 1).

Table 1. Cluster expansions obtained for a description of nanoparticle configurational energies: "bulk" is the bulk CE obtained in Refs. [15,16] without accounting for surface effects; "iso1" and "iso2" ("aniso1" and "aniso2") designate the implementation of isotropic (anisotropic) surface potential affecting one and two external layers, respectively; "100iso1" and "100iso2" are the hybrid CEs for which the surface potential is the same for all (0 0 1) and (1 0 0) types of surfaces but is different from the surface potential for the (1 1 1) surface; and the least-square-fitting (LSF) errors are those of atom exchange energies in two external layers (total and within each surface).

Layers		Cluster expansions						
(lmn)	i	bulk	iso1	iso2	100iso1	100iso2	aniso1	aniso2
		$V^{(1)}_{\mathrm{LCE}} - V^{(1)}_{\mathrm{bulk}}$ (eV)						
(0 0 1)	8	0	−0.33	−0.13	−0.264	−0.065	−0.284	0.102
	7	0	0	0.201	0	0.199	0	0.386
	2	0	0	0.201	0	0.199	0	0.050
	1	0	−0.33	−0.13	−0.264	−0.065	−0.222	−0.172
(1 0 0)	2	0	0	0.201	0	0.199	0	0.160
	1	0	−0.33	−0.13	−0.264	−0.065	−0.284	−0.124
(1 1 1)	2	0	0	0.201	0	0.207	0	0.207
	1	0	−0.33	−0.13	−0.531	−0.324	−0.531	−0.324
		LSF error (eV/at)						
(0 0 1)		0.026	0.021	0.013	0.020	0.012	0.020	0.004
(1 0 0)		0.015	0.009	0.007	0.002	0.006	0.008	0.002
(1 1 1)		0.022	0.011	0.008	0.008	0.003	0.008	0.003
Total		0.023	0.016	0.011	0.015	0.009	0.015	0.003

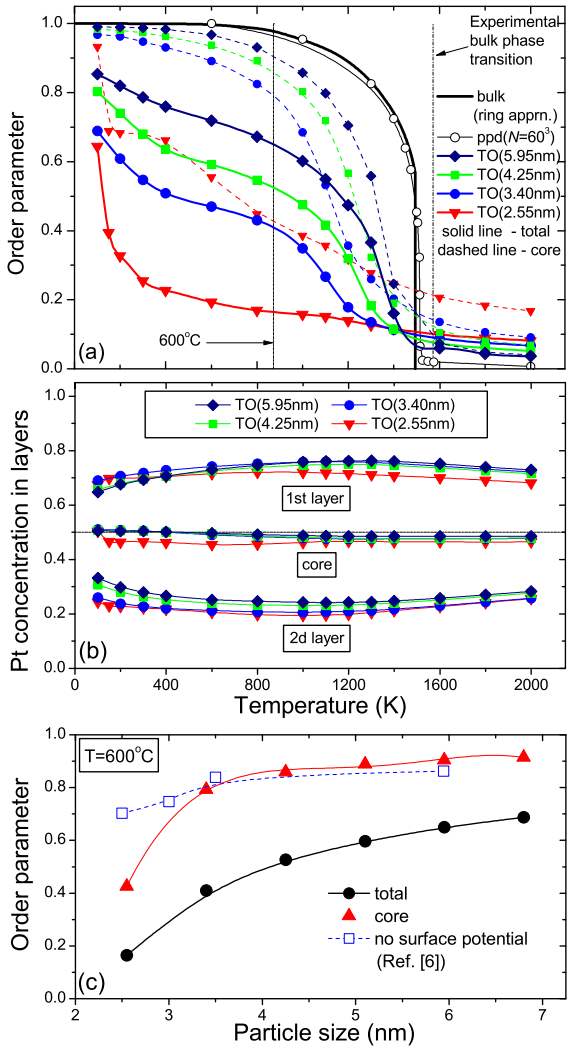

Figures 4. The temperature dependence of the equilibrium (a) $L1_0$ order parameter $\overline{\eta}$ and (b) Pt concentrations in two external layers and internal core for truncated octahedron ("TO") shape nanoparticles with different sizes at near equiatomic composition. In graph (a), we include the data obtained within the analytical ring approximation [40,41] for bulk ("bulk") as well as by Monte Carlo simulation for the parallelepiped ("ppd") sample containing $N = 60^3$ atoms. The solid and dashed lines represent the total and core (excluding two external layers) order parameters, respectively. (c) Equilibrium $L1_0$ order parameters $\overline{\eta}$ vs. particle size at $T = 600$ °C: total, core (excluding two external layers) and obtained in Refs. [15,16] by neglecting surface potential.

The results of our Monte Carlo simulations with the "iso2" cluster expansion are presented in Figure 4. The comparison of the present and previous [15,16] results confirms that the presence of a surface potential reduces the total order in agreement with Refs. [17–20]. The reduction is larger for smaller particles having a bigger fraction of surface vs. volume. In addition, there is a negligible effect of the surface potential on the core order parameter for particles larger than ~3.4 nm, followed by a still considerable total order parameter (~0.4–0.5 of maximum value at 600 °C). Only for particles smaller than ~3.4 nm, is there a strong reduction in order.

Figure 4b shows that the Pt-segregation into the first external layer is compensated by Pt-depletion in the second layer so that the composition of the core remains

close to ideal. This is a direct consequence of the values of the surface potential "iso2" for the two external layers, similar in magnitude but with opposite sign (Fig. 3 and Table 1). Consequently, as the core remains close to stoichiometry, its ordered state is affected by surface thermodynamics less than that previously concluded [17–20].

Our model considers only configurational entropy and neglects other effects. For instance, the effects of vibrational [42] or magnetic [43] entropies are not included. However, the good agreement between the measured and calculated bulk transition temperatures (Fig. 4) suggests that these corrections are small in the important range $T < 600$ °C. Furthermore, we have also considered nanoparticles embedded in vacuum rather than in the polymeric medium typically used. Nevertheless, our surface potential is similar to previous estimates based on experimental data [19,20] and, more importantly, our most crucial observation pertains to the second subsurface atomic layer, which is clearly less sensitive to the surrounding media. Therefore, our findings reopen the possibility that the weak ordering observed experimentally is not due to fundamental thermodynamic limitations but probably to kinetic effects [44] that may be easier to control [15,16].

This research was supported by ONR (N00014-07-1-0878, N00014-07-1-1085, N00014-09-1-0921), NSF (DMR-0639822) and DOE (DE-FG07-071D14893). Computational support was provided by the TeraGrid resources at TACC (MCA-07S005), NCSA and SDSC (TG-DMR050013N).

[1] I.M.L. Billas, A. Châtelain, W.A. de Heer, Science 265 (1994) 1682.
[2] F. Baletto, R. Ferrando, Rev. Mod. Phys. 77 (2005) 371.
[3] M.L. Tiago, Y. Zhou, M.M.G. Alemany, Y. Saad, J.R. Chelikowsky, Phys. Rev. Lett. 97 (2006) 147201.
[4] S. Sun, C.B. Murray, D. Weller, L. Folks, A. Moser, Science 287 (2000) 1989.
[5] H. Zeng, J. Li, J.-P. Liu, Z.L. Wang, S. Sun, Nature 420 (2002) 395.
[6] S. Sun, Adv. Mater. 18 (2006) 393.
[7] S.D. Bader, Rev. Mod. Phys. 78 (2006) 1.
[8] Y.K. Takahashi, T. Ohkubo, M. Ohnuma, K. Hono, J. Appl. Phys. 93 (2003) 7166.
[9] T. Miyazaki, O. Kitakami, S. Okamoto, Y. Shimada, Z. Akase, Y. Murakami, D. Shindo, Y.K. Takahashi, K. Hono, Phys. Rev. B 72 (2005) 144419.
[10] C.B. Rong, D. Li, V. Nandwana, N. Poudyal, Y. Ding, Z.L. Wang, H. Zeng, J.P. Liu, Adv. Mater. 18 (2006) 2984.
[11] J.P. Liu, K. Elkins, D. Li, V. Nandwana, N. Poudyal, IEEE Trans. Magn. 42 (2006) 3036.
[12] S. Kang, S. Shi, Z. Jia, G.B. Thompson, D.E. Nikles, J.W. Harrell, D. Li, N. Poudyal, V. Nandwana, J.P. Liu, J. Appl. Phys. 101 (2007) 09J113.
[13] U. Wiedwald, A. Klimmer, B. Kern, L. Han, H.-G. Boyen, P. Ziemann, K. Fauth, Appl. Phys. Lett. 90 (2007) 062508.
[14] Annealing at ~600 °C results in sintering of nanoparticles into larger agglomerates.
[15] R.V. Chepulskii, J. Velev, W.H. Butler, J. Appl. Phys. 97 (2005) 10J311.
[16] R.V. Chepulskii, W.H. Butler, Phys. Rev. B 72 (2005) 134205.
[17] B. Yang, M. Asta, O.N. Mryasov, T.J. Klemmer, R.W. Chantrell, Scripta Mater. 53 (2005) 417.
[18] B. Yang, M. Asta, O.N. Mryasov, T.J. Klemmer, R.W. Chantrell, Acta Mater. 54 (2006) 4201.
[19] M. Müller, K. Albe, Phys. Rev. B 72 (2005) 094203.
[20] M. Müller, P. Erhart, K. Albe, Phys. Rev. B 76 (2007) 155412.
[21] C. Srivastava, J. Balasubramanian, C.H. Turner, J.M. Wiest, G.B. Thompson, J. Appl. Phys. 102 (2007) 104310.
[22] A.R. Harutyunyan, N. Awasthi, A. Jiang, W. Setyawan, E. Mora, T. Tokune, K. Bolton, S. Curtarolo, Phys. Rev. Lett. 100 (2008) 195502.
[23] S. Curtarolo, N. Awasthi, W. Setyawan, A. Jiangm, K. Bolton, T. Tokune, A.R. Harutyunyan, Phys. Rev. B 78 (2008) 054105.
[24] M.E. Gruner, G. Rollmann, P. Entel, M. Farle, Phys. Rev. Lett. 100 (2008) 087203.
[25] J.M. Sanchez, F. Ducastelle, D. Gratias, Physica 128A (1984) 334.
[26] A. van der Ven, G. Ceder, M. Asta, P.D. Tepesch, Phys. Rev. B 64 (2001) 184307.
[27] A. Van der Ven, G. Ceder, Phys. Rev. B 71 (2005) 054102.
[28] L.D. Marks, Rep. Prog. Phys. 57 (1994) 603.
[29] M.J. Yacaḿan, J.A. Ascencio, H.B. Liu, J.G. Torresdey, J. Vac. Sci. Technol. B 19 (2001) 1091.
[30] Z.R. Dai, S. Sun, Z.L. Wang, Surf. Sci. 505 (2002) 325.
[31] Y. Wang, J.P. Perdew, Phys. Rev. B 44 (1991) 13298.
[32] G. Kresse, J. Furthmüller, Comput. Mater. Sci. 6 (1996) 15.
[33] All ferromagnetic structures were fully relaxed (cell shape and volume and atom cell-internal positions) but preserving the empty space between the slabs. Numerical convergence to within about 1 meV atom^{-1} is ensured by enforcing a high energy cut-off (400 eV) and dense ($14 \times 14 \times 2$ and $15 \times 7 \times 1$) Monkhorst–Pack k-point meshes.
[34] A.V. Ruban, H.L. Skriver, J.K. Nørskov, Phys. Rev. B 59 (1999) 15990.
[35] A.U. Nilekar, A.V. Ruban, M. Mavrikakis, Surf. Sci. 603 (2009) 91.
[36] P. Beccat, Y. Gauthier, R. Baudoing-Savois, J.C. Bertolini, Surf. Sci. 238 (1990) 105.
[37] R. BaudoingSavois, Y. Gauthier, W. Moritz, Phys. Rev. B 44 (1991) 12977.
[38] R.M. Wang et al., Phys. Rev. Lett. 100 (2008) 017205.
[39] K.L. Torres, G.B. Thompson, Ultramicroscopy 109 (2009) 606.
[40] R.V. Chepulskii, Solid State Commun. 115 (2000) 497.
[41] R.V. Chepulskii, Phys. Rev. B 69 (2004) 134431.
[42] A. van de Walle, G. Ceder, Rev. Mod. Phys. 74 (2002) 11.
[43] A.V. Ruban, I.A. Abrikosov, Rep. Prog. Phys. 71 (2008) 046501.
[44] A possible experimental confirmation of the conclusion can be made based on the data of [11–13], in which it was shown that the atomic order can be increased by NaCl treatment, ion irradiation, and by increase of temperature and/or annealing time, indicating underlying kinetic issues.